Resonant Rydberg-atom–Rydberg-atom collisions

T. F. Gallagher, K. A. Safinya,* F. Gounand,† J. F. Delpech,‡ W. Sandner,§ and R. Kachru
Molecular Physics Laboratory, SRI International, Menlo Park, California 94025
(Received 16 November 1981)

The experimental investigation of the resonant collision process Nans + Nans → Nanp + Na$(n-1)p$ which occurs when the levels are tuned with an electric field so that the ns level lies midway between the two p levels is described in detail. The observations are shown to be in good agreement with a long-range resonant dipole-dipole interaction.

I. INTRODUCTION

Resonant collisional energy transfer, the process in which atom (or molecule) A loses as much internal energy as its collision partner atom (or molecule) B gains, is a process which has been of interest for some time. While it has been studied theoretically in some detail, both for atomic and molecular collisions,[1–3] the experimental exploration of this subject has been hindered by the necessity of finding chance coincidences in the separations of the energy levels of the collision partners. In spite of this obstacle considerable insight has been gained into the nature of resonant collisions using the available coincidences.[4,5]

The study of resonance effects in collisions is greatly facilitated by the use of Rydberg atoms. First there is a high probability of finding chance coincidences because of the systematic variation of the energy separations with principal quantum number n and orbital angular-momentum quantum number l. This allows much more systematic studies than were previously possible. For example, the variation of energy separation with n produces a comb of allowed transition frequencies which is nearly continuous in some spectral regions, and this has been used to probe resonance effects in electronic to rotational and vibrational energy transfer.[6–8] Using the resulting discrete step tuning it has been possible to determine the widths of these collisional resonances to be 6 cm^{-1} and 50 cm^{-1}, respectively, although the exact widths are somewhat uncertain due to the comb-like nature of the energy spacing. It is interesting to note that in both these cases, at resonance the cross sections are slightly smaller in size than the geometric size of the Rydberg atom, and the dominant interaction in these collisions is thought to be the quasifree *electron* scattering of the Rydberg electron from the perturbing atom or molecule.

Since Rydberg atoms have large dipole moments their energies are easily shifted by the application of very modest electric fields thus allowing the study of resonant collisions with continuous tuning. Previously we described the first application, to our knowledge, of such an approach to study resonant collisions of two Rydberg atoms.[9] We notice that in nuclear magnetic resonance, magnetic field tuning has been used to observe roughly analogous resonant energy transfer between nuclear spins in solids.[10] Although several mechanisms are responsible for the observed effects, such processes are frequently termed cross relaxation.[10]

Specifically, we have studied the sharply resonant thermal-collision process Na $ns + ns \rightarrow np + (n-1)p$ which occurs when the Na ns levels are tuned with an electric field so that the ns level lies midway between the two p states. As shown by Fig. 1 for the 17s, 16p, and 17p states, there are in fact four collisional resonances due to the splitting of $|m_l| = 0$ and 1 levels in the electric field. We shall designate the four resonances by the $|m_l|$ levels of the lower and upper p states, respectively. Thus in order of increasing field the four resonances are (0,0), (1,0), (0,1), and (1,1).

Cross sections $\sim 10^3$ times greater than the geometric cross sections of the atoms with resonance widths of ~ 0.03 cm^{-1} were observed. Both of these striking features are consequences of the large dipole moments of the Rydberg atoms which allow an efficient long-range resonant dipole-dipole interaction. Such an interaction was termed a "rotational resonance" by Anderson,[2] and has been observed, although not systematically, in molecular resonant rotational energy transfer.[4]

It is our purpose here to give a more detailed description of the experimental approach and observations as well as a simple treatment of resonant collisions.

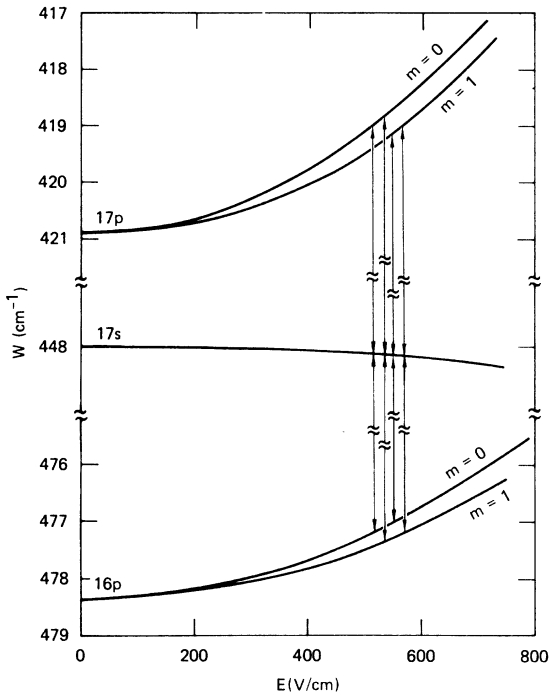

FIG. 1. Energy-level diagram for the 16*p*-17*s*-17*p* states in a static electric field. The vertical lines are drawn at the four fields where the *s* state is midway between the two *p* states and the resonance collisional transfer occurs.

II. RESONANT COLLISIONS

Since the formal theory of long-range dipole-dipole collisions has been developed from the scattering point of view and can be found in several places,[1] there is little point in repeating such a treatment here. Rather we present two treatments derived from radio-frequency spectroscopy. The first is an order-of-magnitude argument derived from Purcell's[11] treatment of electron-collision-induced hydrogen 2*s*-2*p* transitions. The second more elaborate treatment serves mainly to produce an explicit analytic expression for the width of the collisional resonances. In both we use atomic units.

The treatment based upon Purcell's work gives quickly the approximate values of the cross sections and resonance widths. Imagine that we have two two-state atoms 1 and 2, one in its upper and one in its lower state, which have transition matrix elements μ_1 and μ_2 for transitions at the same frequency ω. Further, these atoms pass each other with relative velocity v and impact parameter b as shown in Fig. 2. Atom 1 may be viewed as a classical dipole of magnitude μ_1, rotating at frequency ω. This produces an oscillating field E at atom 2 the magnitude of which is given by

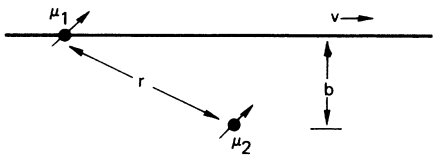

FIG. 2. Geometry of the collision of two dipoles. μ_2 is at rest and μ_1 passes with velocity v and impact parameter b. The dipoles are separated by r.

$$E \sim \frac{\mu_1}{r^3} , \tag{1}$$

where r is the distance between the atoms. For this field to induce a transition of atom 2

$$\mu_2 E t \sim 1 , \tag{2}$$

where t is the interaction time. Since E is only appreciable when $r \sim b$, we may use $E = \mu_1 / b^3$ and $t = b/v$ in Eq. (2) and rewrite Eq. (2)

$$\frac{\mu_1 \mu_2}{b^2 v} \sim 1 . \tag{3}$$

This yields the value of the impact parameter for which the resonant-energy transfer will occur with unit probability. Thus

$$\sigma \sim b^2 = \frac{\mu_1 \mu_2}{v} . \tag{4}$$

Similarly the width of the resonance $1/t$ is given by

$$1/t \simeq \left[\frac{v^3}{\mu_1 \mu_2} \right]^{1/2} . \tag{5}$$

Since for these Rydberg transitions $\mu_1 \approx \mu_2 \approx n^2$, then Eqs. (4) and (5) can be written as

$$\sigma = \frac{n^4}{v} \tag{6}$$

and

$$1/t = \frac{v^{3/2}}{n^2} . \tag{7}$$

Thus the cross section scales as n^4 and the interaction time as n^2.

In atomic units the thermal velocity $v \sim 10^{-4}$, thus the cross sections are $\sim 10^4$ times larger than the geometric cross sections. In more familiar units, at $n = 20$, $\sigma \sim 10^9$ Å^2 and $t \sim 1$ nsec.

The fact that we are able to sweep through the collisional resonance suggests that we treat the problem in such a way that the resonant behavior emerges in much the same way it does in treatments of radio-frequency resonance. Accordingly, the following discussion, which leads to a simple expression for the width of the resonances, draws heavily upon the two-state magnetic resonance treatment of Ramsey,[12] and is formally identical to the perturbation treatment of Kleppner.[13]

Consider two colliding atoms as shown in Fig. 3. One of the atoms is assumed to be stationary at the origin and the other, passing the first atom with an impact parameter b at $x=0$, is moving in the x direction, perpendicular to the page, with velocity v. We shall assume that the second atom travels in a straight line and is not deflected by the collision. In addition we shall assume that there is a static electric field in the z direction. This choice of axes matches our experimental configuration. We construct the product states

$$\psi_A=\psi_1 ns\,\psi_2 ns\ , \tag{8a}$$

$$\psi_B=\psi_1 np\,\psi_2(n-1)p\ , \tag{8b}$$

where ψnl describes a Stark-state wave function that is adiabatically connected to the corresponding zero-field n,l Coulomb wave function. The total wave function for the system may be written as

$$\psi(t)=\psi_A C_A(t)+\psi_B C_B(t)\ , \tag{9}$$

where all the time dependence is in the coefficients $C_A(t)$ and $C_B(t)$. The energies of the two states A and B at $r=\infty$, where r is the internuclear separation, are given by

$$W_A=W_{ns}+W_{ns}\equiv 0 \tag{10a}$$

and

$$W_B=W_{np}+W_{(n-1)p}\ , \tag{10b}$$

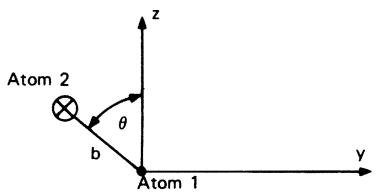

FIG. 3. Geometry of the collision of two atoms. Atom 1 is at rest at the origin. Atom 2 is moving in the x direction, perpendicular to the paper, with velocity v and impact parameter b. At $x=0$, the plane of the paper, the vector from atom 1 to atom 2 makes an angle θ with the z axis, the axis of quantization.

which we take to be the eigenvalues of the unperturbed Hamiltonian H_0 of two noninteracting (infinitely separated) atoms in the static electric field. For finite internuclear separations the states A and B are coupled by the dipole-dipole interaction

$$\langle\psi_A\mid V\mid\psi_B\rangle=\left\langle\psi_A\left|\frac{\vec{\mu}_1\cdot\vec{\mu}_2}{r^3}-\frac{3(\vec{\mu}_1\cdot\vec{r})(\vec{\mu}_2\cdot\vec{r})}{r^5}\right|\psi_B\right\rangle . \tag{11}$$

Here $\vec{r}$ is the vector between the two atoms.

Strictly speaking the assumption of an undeflected path for the moving atom does not allow the (0,1) or (1,0) resonances, as the change in the orbital angular momentum must come from the translational motion. However, because of the large impact parameter the amount of energy transferred is negligible, $\sim 1.6\times 10^{-3}$ cm^{-1}. Thus the approximation of undeflected paths is quite good.

The interaction matrix elements may be simplified by taking the RMS value of Eq. (11) over the angle θ in Fig. 3. This yields for the (0,0) transition

$$\langle\psi_A\mid V\mid\psi_B\rangle=\frac{\langle ns\mid\mu_1\mid np\rangle\langle ns\mid\mu_2\mid n-1p\rangle}{r^3}\ , \tag{12}$$

that is the product of the two dipole-matrix elements divided by r^3. Similar expressions are obtained from the other resonances.

Inserting the wave function of Eq. (9) and the Hamiltonian H_0+V yields the pair of equations

$$i\dot{C}_A=W_A C_A(t)+VC_B(t)\ , \tag{13a}$$

$$i\dot{C}_B=V^* C_A(t)+W_B C_B(t)\ . \tag{13b}$$

For V real and $W_A=0$, this may be recast in the form

$$i\ddot{C}_A+\dot{C}_A\frac{\dot{V}}{V}=V^2 C_A+iW_B\dot{C}_A\ . \tag{14}$$

Recall from Eq. (12) the form of the matrix element V. It is nearly zero everywhere except where $r=b$, where it reaches a maximum. Inspection of a graph of V vs x suggests the approximation

$$V=\begin{cases}\dfrac{\chi}{b^3} & \text{for } -\dfrac{b}{2}<x<\dfrac{b}{2}\\ 0 & \text{elsewhere}\ .\end{cases} \tag{15}$$

Here $\chi=\langle ns\mid\mu_1\mid np\rangle\langle ns\mid\mu_2\mid(n-1)\mid p\rangle$. This makes the $\dot{V}/V$ term $\equiv 0$ and suggests choosing the time origin so that the interaction time is $0<t<b/v$. Thus the problem is reduced to pre-

cisely the magnetic resonance problem described by Ramsey.[12]

Initially both atoms are in the s state, thus $C_A(0)=1$ and $C_B(0)=0$. With these initial conditions, for $0<t<b/v$, C_A and C_B are given by

$$C_A(t)=\left[\cos\left[\frac{\alpha t}{2}\right]\frac{-iW_B}{\alpha}\sin\left[\frac{\alpha t}{2}\right]\right]\times\exp(iW_B t/2) \tag{16}$$

and

$$C_B(t)=\frac{-i2\chi}{b^3\alpha}\sin\left[\frac{\alpha t}{2}\right]\exp(iW_B t/2)\ , \tag{17}$$

where $\alpha=(W_B^2+4\chi^2/b^6)^{1/2}$. The probability P of finding the atoms in the two p states is given by $C_B^2(b/v)$. Thus we may write the probability as

$$P=\frac{4\chi^2/b^6}{W_B^2+4\chi^2/b^6}\sin^2\frac{1}{2}\left[W_B^2+\frac{4\chi^2}{b^6}\right]^{1/2}\frac{b}{v}\ . \tag{18}$$

For $P=1$ at resonance ($W_B=0$) this defines an impact parameter b_0:

$$b_0^2=2\chi/\pi v\ . \tag{19}$$

The cross section is given by

$$\sigma=\int_0^\infty 2\pi bP(b)db\ . \tag{20}$$

Taking $P=\frac{1}{2}$ for $b<b_0$ to approximate the rapid oscillations and numerically integrating Eq. (20) for $b>b_0$, we find

$$\sigma=2.3\pi b_0^2 \tag{21}$$

in good agreement with Anderson's result which is[2]

$$\sigma=\pi^2(\tfrac{8}{9})b_0^2\ . \tag{22}$$

From Eqs. (18) and (19) it is apparent that the width of the resonances is given by

$$\Delta(\text{FWHM})=\frac{4\chi}{b_0^3}=\frac{2\pi v}{b_0}=\left[\frac{2\pi^3v^3}{\chi}\right]^{1/2}, \tag{23}$$

which is in good agreement with the result of van Kranendonk,[3]

$$\Delta(\text{FWHM})=5v/b_0\ , \tag{24}$$

for dipole-dipole collisions if we make the reasonable approximation that $1/b_0$ is the average value of $1/b$. We notice that in our treatment the maximum probability occurs exactly on resonance, at $W_B=0$, whereas in the treatment of van Kranendonk it occurs for $W_B\neq 0$. This difference comes from the fact that we have discarded the term containing $\dot{V}/V$ in Eq. (14).

To evaluate the cross sections and collision widths we must use the actual values of the average collision velocity $\bar{v}=1.6\times10^{-4}$ and dipole moments $\mu_1=\mu_2=0.60n^{*2}$. Here n^{*2} is the effective quantum number of the ns state of binding energy $W=-1/2n^{*2}$. Using our results, Eqs. (21) and (22), these values lead to cross sections and widths (FWHM) given by

$$\sigma=1.03\times10^4 n^{*4} \tag{25}$$

and

$$\Delta=2.64\times10^{-5}n^{*-2}\ . \tag{26}$$

In laboratory units

$$\sigma=2.90\times10^3 n^{*4}\ \text{Å}^2 \tag{27}$$

and

$$\Delta=1.74\times10^2 n^{*-2}\ \text{GHz}\ . \tag{28}$$

III. EXPERIMENTAL APPROACH

In the experiment, an effusive beam of Na passes between a plate and a grid as shown in Fig. 4 where it is excited in two steps by two pulsed dye lasers, the first, yellow laser, tuned to the $3s$-$3p$ transition at 5890 Å, and the second, blue laser, tuned to the $3p$-ns transition at $\sim$4140 Å. The laser excitation and subsequent collisions occur in a dc electric field which ranges from 80–800 V/cm in these experiments. At a variable time after the

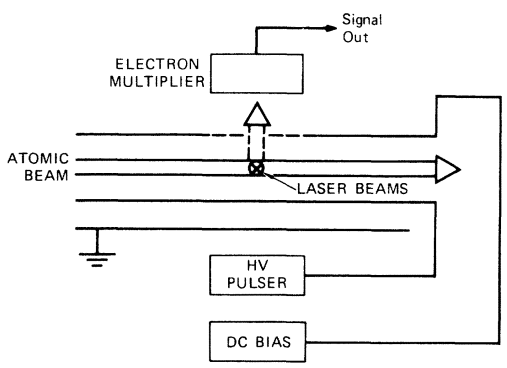

FIG. 4. The interaction region of the apparatus, showing both laser beams perpendicular to the atomic beam.

laser excitation a positive high-voltage pulse is applied to the plate field ionizing the Rydberg atoms and accelerating the resulting ions into the electron multiplier. The electron multiplier signal is averaged using a boxcar averager and recorded with a chart recorder.

The selectivity of electric field ionization enables us to identify states present at the time the field-ionizing pulse is applied. In this work we chiefly use the temporal resolution of ion signals from different states at a fixed ionizing-field amplitude. As noted previously, it is possible to discriminate between states of different n, l, and $|m_l|$ using this technique.[14] Thus we are able to monitor the populations in the ns, np, and $(n-1)p$ states as functions of time after the laser pulse an dc electric field.

Although most of the details of the experimental apparatus may be found elsewhere[13] we note here points of particular importance for this experiment. First, the atomic beam is collimated to a 0.4-cm diameter in the interaction region, has a density of $\sim 10^8$ cm^{-3}, and is assumed to have the modified Maxwellian velocity distribution characteristic of a 500 °C beam.

The laser beams are focused to 0.5-mm diameter in the interaction region, are usually approximately collinear, and cross the atomic beam at right angles as shown in Fig. 4. To vary the excitation volume the blue laser is sometimes introduced along the atomic-beam axis counterpropagating to the atomic beam. With both laser beams crossing the atomic beam at 90° the excitation volume is a cylinder of volume 10^{-3} cm^3. Typical densities of excited atoms are $\sim 10^6$ cm^{-3}.

The electron multiplier gain is measured to be 5×10^{-3}, and has a specified quantum efficiency of 30%. Including the 20 db (power) gain of the amplifier after the multiplier, we find that overall, one Rydberg atom leads to $\sim 1.9\times 10^{-15}$ C of signal.

IV. OBSERVATIONS

A. Qualitative observations

Before describing in detail the cross-section measurements it is useful to present qualitative observations which both identify the collision process and suggest the method used to measure the cross sections. The most striking feature of our observations is the sharply resonant increase in the populations when the levels are tuned into resonance with the field. An example is shown in Fig. 5, a recording of the population in the $17p$ state as a function of dc field 2 μsec after the $17s$ state is populated by the lasers. The sharp increases in signal at 516, 537, 544, and 566 V/cm are due to the resonant $17s + 17s \rightarrow 16p + 17p$ collisions which occur as shown in Fig. 1. As mentioned earlier, the resonances are labeled by the $|m_l|$ values of the final lower and upper p states, which are determined from the field-ionization behavior of the signal in the lowest n states studied. Since the field-ionization identification for the lowest n states is consistent with the energy levels of Fig. 1, we assumed this to be true for all n values we studied. In addition, the resonant signal is approximately quadratic in the power of the blue laser, whereas the total population is linear, as shown by Fig. 6. This suggests that the resonant signal is either due to an effect which depends upon collisions with photoions produced by the absorption of two blue-laser photons or to an effect varying as the square of the number of excited atoms. Since there are no photoions observed we can immediately rule out the first possibility. Considering the small size of photoionization cross sections for Rydberg atoms by visible photons[15] and the likelihood of a resonant process this seems unlikely in any case.

Thus the process must be either a collision between two excited atoms or some sort of cooperative effect involving the ns, np, and $(n-1)p$ states—such as superradiance. Since superradiance occurs quite easily in Rydberg-atom systems,[16] it is interesting to consider the possibility of a coopera-

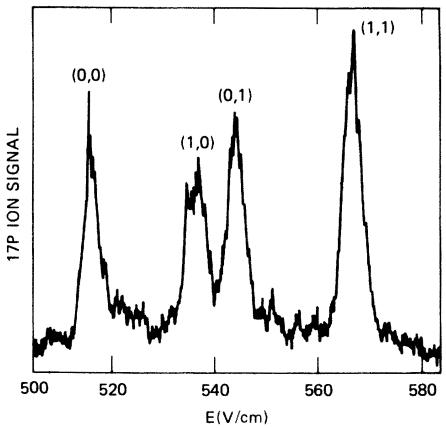

FIG. 5. The observed $17p$ ion signal after population of the $17s$ state vs dc electric field, showing the sharp collisional resonances. The resonances are labeled by the $|m_l|$ values of the lower and upper p states.

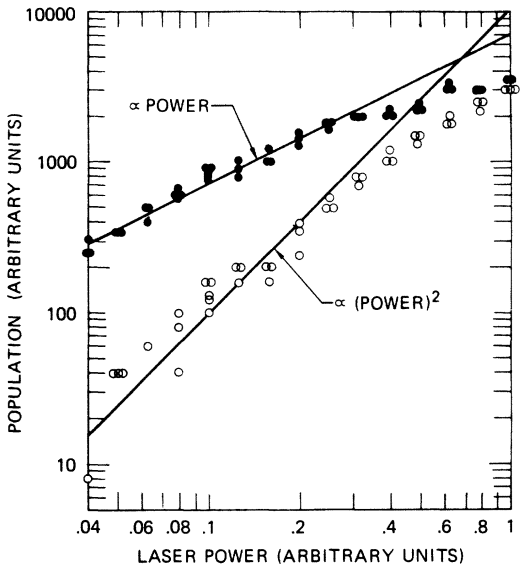

FIG. 6. The blue-laser-intensity dependence of the $17p$ resonant collision signal (○) and $17s$ signal (●) after population of the $17s$ state showing the quadratic dependence of the resonant signal.

tive phenomenon to show why we have ruled it out in this case. For a cooperative effect to occur a macroscopic dipole must be set up in the medium and the effect must occur in a time short compared to the relaxation times.[17]

In a two-level Rydberg-atom system prepared entirely in the upper level the dipole is usually established by amplified blackbody radiation. Whether or not the dipole is actually established is determined by the amplification or gain of the sample for the transition under study.[16] Typically there must be a gain of ~ 1 in the sample. Stated another way, in traversing the sample a photon at the correct frequency has a probability of one of inducing an atom to emit a second photon. This occurs when $n_u \sigma_0 l \sim 1$, where n_u is the number density of atoms in the upper state, σ_0 is the optical cross section, and l is the sample length. This requirement is easily met by the zero electric field Nans states, for example, because of the large, $\sim n^2$, dipole moments connecting them to the $(n-1)p$ states. Under this circumstance the thermal blackbody radiation is amplified and establishes the macroscopic polarization. In the electric field case we are considering here in which the transitions ns-np and ns-$(n-1)p$, absorption and stimulated emission, respectively, are at the same frequency, and whether there is gain or absorption depends upon the magnitude of the dipole-matrix elements. Since they are the same to within a few percent in this case, there is apparently no net gain to establish the macroscopic dipole.

Even though, in principle, it appears impossible for a cooperative effect to occur we have a direct experimental check, the time scale of the observed effects. In zero field the Nans states exhibit superradiance in times <300 nsec after the laser pulse. We never observe a time delay greater than 300 nsec indicating that the relaxation times are <300 nsec. When we begin to apply a dc field we find that the superradiance disappears at 50 V/cm for $16s$ and 3 V/cm for $20s$. We attribute the decrease in superradiance in these fields, which are ten times smaller than the fields in which the resonant collisions occur, to a diminishing of the ns-$(n-1)p$ matrix element with the electric field and broadening by electric field inhomogeneities. For $27s$ we never observe superradiance. In this connection it is interesting to note that as n goes from 16 to 27 the wavelength of the $ns \rightarrow (n-1)p$ transition increases from 0.3 to 1.6 mm, i.e., from smaller than the sample size to larger than the sample size. It has been suggested that under such circumstances superradiance will not occur because of the direct dipole-dipole interaction between the atoms.[18,19]

From the considerations above it is clear that in the field the relaxation times are certainly less than 300 nsec, and if the effect is cooperative it must occur faster than 300 nsec. However, that is not the case as shown by Fig. 7 which shows the time evolution of the $20p$ signal after the laser excitation of the $20s$ state for the on- and off-resonant cases. As shown by Fig. 7 the resonant increase in the population of the $20p$ state occurs over a 1-μsec period (determined by the sample geometry), certainly not in a time fast compared to 300 nsec. (The fact that the nonresonant signal is not zero at $t=0$ indicates that we are partially ionizing the parent $20s$ state as well; however, this has no effect upon our conclusions.)

To investigate whether number or number density of excited atoms was important, we introduced the blue laser along the atomic beam, perpendicular to the yellow laser, so as to excite a smaller number of atoms but the same number density. We found the relative magnitudes of the resonant and nonresonant signals to be the same. Equivalently, if when the laser beams are parallel the blue laser is attenuated to produce the same initial number of $20s$ atoms as are produced with the laser perpendicular, the resonant signal is proportionally much smaller. These observations indicate

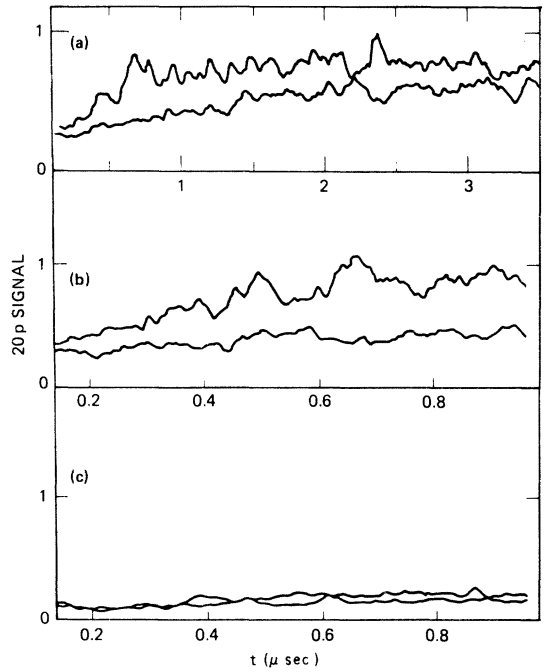

FIG. 7. Time dependence of the $20p$ signal after the population of the $20s$ state with the two laser beams parallel to each other. In each case the upper trace is on and the lower is off resonance. Thus, the difference is the buildup of the resonant collision signal. The off-resonance signal at $t \sim 0$ is from partial ionization of the $20s$ state. (a) A scan of ~ 4 μsec showing the 1-μsec time scale of the process. (b) A scan of ~ 1 μsec showing the early development of the signal. (c) A scan of ~ 1 μsec with the laser power reduced to 40% of that used in (b). Notice the drastic reduction of the resonant signal.

that the effect depends upon the number density of Rydberg atoms as expected for a collision process. When the above observations are considered together it is difficult to imagine that the process is cooperative, not collisional.

B. Measurement of the cross sections

If we allow collisions to occur for a time T (not to be confused with the collision time t) during which time a small fraction of the initial population in the ns state is collisionally transferred to the np and $(n-1)p$ states then the population N_p in the np (and $n-1)p$ state will be given by

$$N_p = \frac{N_s^2 \sigma \bar{v} T}{V} , \tag{29}$$

where $\bar{v}$ is the average collision velocity, σ is the cross section for the process, V is the sample volume, and N_s is the initial ns state population.

Equation (29) may be easily inverted to give the cross section. In doing so it is convenient to replace N_s and N_p by the signals we observe N_s' and N_p' which are related to N_s and N_p by Γ the overall sensitivity, given in Sec. III. Thus we may write

$$\sigma = \frac{N_p'}{N_s'^{\,2}} \left\{ \frac{V}{\Gamma \bar{v} T} \right\} . \tag{30}$$

By measuring the ratio $N_p'/N_s'^{\,2}$ as a function of n we may determine with good accuracy the n dependence of the cross section. Measurements of the quantities in curly brackets give the absolute cross sections.

Basically the cross-section measurement consists of measuring N_p the population in the np state, and N_T, the total population in np, ns, and $(n-1)p$ states, as the dc electric field is swept through the collisional resonances. Specifically, we field ionize the atoms 2 μsec after the laser pulse and set the amplitude of the ionizing field so that all the ns, np, and $(n-1)p$ states are ionized, with the $(n-1)p$ state being just barely ionized. Because of the large difference in the fields at which the Na ns and np states ionize these two are in all cases easily time resolved. Owing to the small difference in the fields at which the ns and $(n-1)p$ state ionize these are not always clearly resolved under these conditions; however, this has no effect on the determination of the cross sections. With a 50-nsec wide gate we observe only the np state signal, which comes first, yielding N_p', and with a 500-nsec wide gate we observe at the same time the entire ion signal N_T from the np, ns, and $(n-1)p$ states. A typical example of a sweep through the collisional resonances is shown in Fig. 8 for the excitation of the $23s$ state for two laser powers. Figures 8(a) and 8(b) are recordings of N_{23p}', the number of atoms in the $23p$ state at two laser powers. Figures 8(a') and 8(b'), in the inset, show the corresponding simultaneous measurements of N_T', the number of atoms, in the $22p$, $23s$, and $23p$ states, which is clearly unaffected by the collisional resonances. In Figs. 8(a) and 8(b) the quadratic dependence of the resonant signal on blue-laser power is quite apparent, whereas the background (nonresonant) signal in Figs. 8(a) and 8(b) as well as the signal in Figs. 8(a') and 8(b') is clearly linear. Figures 8(a) and 8(b) were obtained on sweeps of increasing and decreasing field, respectively, which leads to apparent slight offsets

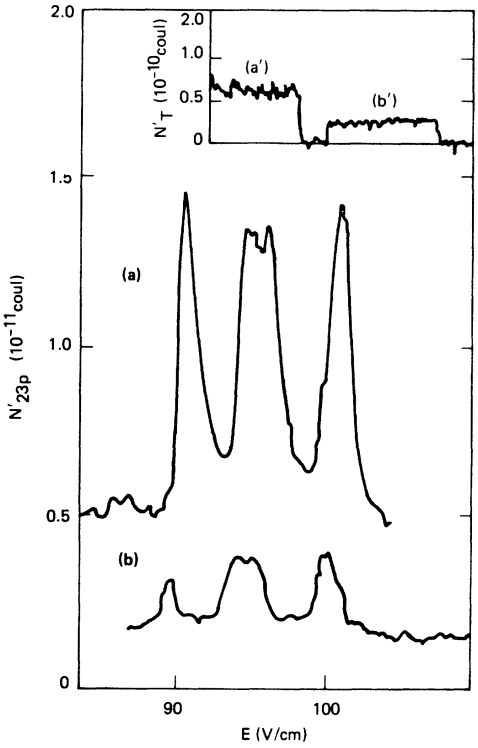

FIG. 8. (a) The population of the 23*p* state 2 μsec after the population of the 23*s* state showing the collisional resonances. Notice that the (0,1) and (1,0) resonances are not resolved in this trace. (b) The same as (a) except with 40% of the blue-laser power. (a') A recording of the total populations in the 23*s*, 22*p*, and 23*p* states taken simultaneously with (a). (b') A recording of the total populations in the 23*s*, 22*p*, and 23*p* states taken simultaneously with (b).

in the positions of the resonances due to the time constant of the signal averager. Where necessary we averaged positions obtained with increasing and decreasing field sweeps to obtain the positions of the resonances. Data such as Fig. 8 were taken for at least two laser powers for each state. Quantities of particular interest are the locations of the resonances, their widths, and the ratio of the signal N_p' to the signal N_T'.

In Table I we give the values of the electric field positions at which the resonances occur. In Fig. 9 we show the n dependence of the positions of the (0,0) and (1,1) resonances, whose locations are given by

$$E_R(0,0)=1.21(2)n^{*-5.34(5)}\ \text{V/cm} \tag{31a}$$

and

$$E_R(1,1)=1.42(2)n^{*-5.35(5)}\ \text{V/cm}\ . \tag{31b}$$

The field widths (FWHM) of the resonances are given in Table II. We are reasonably confident that these widths, which are $\sim 1\%$ of the applied fields, are not appreciably broadened by spatial inhomogeneities in the applied dc field because the widths appear the same whether the blue laser is brought into the interaction region parallel or perpendicular to the yellow laser, thus radically changing the volume occupied by the sample of excited atoms.

Physically it is the frequency width of the resonances in which we are really interested, and we have used an approximate method, based on a suggestion of Cooke,[20] outlined in the Appendix to make the conversion. The frequency widths of the resonances are given in Table III. The widths of the resonances are the sum of the collisional width and unresolved fine structure as shown in Fig. 10. Note that the $|m_l|=1$ states are split by Δ_{fs} which is given by

$$\Delta_{fs}=\frac{\Delta_{fs0}}{3}k\ , \tag{32}$$

where Δ_{fs0} is the fine-structure interval of the

TABLE I. Positions of the resonances (V/cm).

State	Resonance 0,0	0,1	1,0	1,1
16*s*	741(15)	770(15)	781(15)	813(16)
17*s*	516(10)	537(10)	544(10)	566(10)
18*s*	364(8)	387(8)	393(8)	405(8)
20*s*	201(4)	210(4)	214(4)	222(4)
23*s*	91(2)	94.5(20)	95.9(20)	100(2)
25*s*	56.5(13)	59.0(13)[a]		63.1(14)
27*s*	36.6(8)	38.7(8)[a]		41.4(8)

[a]The average location of the unresolved 0,1 and 1,0 resonances.

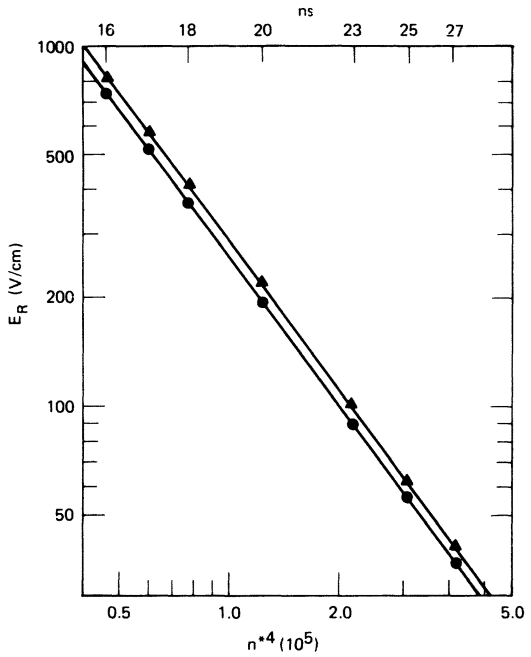

FIG. 9. The positions of the 0,0 (●) and 1,1 (▲) resonances.

zero-field p state and k is the amount of p character remaining in the nominal p state in the electric field. At these fields $k \sim 0.85$ and 0.73 for the lower and upper p state, respectively. From Fig. 10 it is clear that only the (0,0) resonance reflects only the collisional width, the other resonances have additional width from the unresolved fine structure. The (0,1) and (1,0) resonances should each be broader by an amount $\Delta_{\text{fs upper}}$ and $\Delta_{\text{fs lower}}$, respectively. Similarly, the additional width of the (1,1) resonance would be $\Delta_{\text{fs upper}}+\Delta_{\text{fs lower}}$, scaling as n^{-3}. Here we are implicitly assuming that there is no observable spin selection effect, which seems reasonable in view of the fact that we do not specify the spins of the s state atoms. In Fig. 11 we plot the difference in the observed widths, $\Delta(1,1)-\Delta(0,0)$ vs n^{*4} and show the calculated value of $\Delta_{\text{fs upper}}+\Delta_{\text{fs lower}}$ which is in good agreement with the data. In calculating $\Delta_{\text{fs upper}}$ and $\Delta_{\text{fs lower}}$ we have used the previously determined np fine-structure intervals.[21]

From the previous discussion it is clear that the (0,0) resonance is the only good probe of the collision width. The n^* variation of the width of the (0,0) resonance (FWHM) is given by

$$\Delta(0,0)=235(40)n^{*-1.95(20)}\ \text{GHz}\ . \tag{33}$$

In Fig. 12 we plot the observed widths of the (0,0) resonance and calculated dependence from Eq. (26). Note that $\Delta(0,0)$ scales as $n^{*1.9}$, in agreement with the predicted n^{*2} scaling, and is in reasonable agreement with the calculated magnitude.

The cross sections themselves are taken from the ratios $N_p'/N_s'^2$. For N_p' we use the height of the resonances above the flat background signal in recordings such as Figs. 8(a) and 8(b). The average value of N_s' while collisions are occurring is obtained by extrapolating the observed N_T' signal back to 0.5 μsec after the laser pulse, the middle of the time interval during which collisions occur. For the extrapolation we use the 0 K radiative lifetime,[22] not the 300 K radiation decay rate of the ns states since in addition to the ns state we detect the np and $(n-1)p$ states which account for $>80\%$ of the blackbody radiation induced decay of the ns state.[23] In some of the higher-lying states, at the highest laser powers used the resonant collisions were depleted the s state by 30% in which case Eq. (30) is not valid and we used an expansion of which Eq. (30) is the leading term. To simplify the presentation we have corrected the observed $N_p'/N_s'^2$ ratios to account for depletion and present them in Table IV along with the radiative lifetimes of the ns states. The $N_p'/N_s'^2$ ratios are proportional to the cross sections and give the variation of the cross sections with n.

TABLE II. Field widths of the resonances (V/cm).

	Resonance			
State	0,0	0,1	1,0	1,1
16s	4.0(8)	6.7(14)	4.6(9)	7.2(14)
17s	3.4(7)	4.8(10)	4.2(8)	5.3(11)
18s	2.7(6)	4.0(8)	3.6(8)	3.9(8)
20s	1.8(4)	2.7(4)	2.7(5)	2.4(5)
23s	1.35(50)			1.45(30)
25s	0.8(2)			1.15(22)
27s	0.55(20)			0.67(140)

TABLE III. Frequency widths of the resonances (GHz).

State	Resonance 0,0	0,1	1,0	1,1
16*s*	1.11(25)	1.95(50)	1.32(34)	2.31(6)
17*s*	1.08(23)	1.53(40)	1.34(40)	1.70(42)
18*s*	0.94(20)	1.45(35)	1.31(40)	1.52(38)
20*s*	0.77(16)	1.19(30)	1.19(30)	1.08(27)
23*s*	0.74(16)			0.88(22)
25*s*	0.50(12)			0.81(20)
27*s*	0.40(10)			0.51(13)

By evaluating the quantity in the braces of Eq. (30) we obtain absolute values for cross sections. The values used are $\Gamma=5.2\times10^{14}$ atoms/C, $T=1$ μsec, $\bar{v}=3.5\times10^{4}$ cm/sec, and $V=10^{-3}$ cm^3. We estimate the errors in this normalization to be at most of a factor of 5. With the error bars of the relative cross sections from table IV, the observed cross sections can be expressed as

$$\sigma=3.3(6)\times10^{4}n^{*3.7(5)}\ \text{Å}^2\ , \tag{34}$$

which is in good agreement with the calculated values of Sec. II. In Fig. 13 we plot the observed cross sections and the theoretical result, Eq. (27) logarithmically vs n^{*4}.

VI. CONCLUSION

The observed resonant-collision process is perhaps one of the best examples of resonant dipole-dipole collisions with little contribution from higher multipole or hard-sphere effects. As such it is of interest from a fundamental point of view because it is theoretically tractable and experimentally very accessible. For example, systematic studies of the collisional resonances involving the manifold of Stark states should allow one to probe the effect of varying dipole moments without changing the size of the atom. In addition the long time duration of the collision, ~1 nsec, and the large dipole moments imply that it should be straightforward to study perturbations of the collisions. For example, using microwaves it should be possible to do experiments analogous to laser-induced collision experiments.[24] Finally we notice that the magnitude of the collision cross sections suggests that they must be considered in applica-

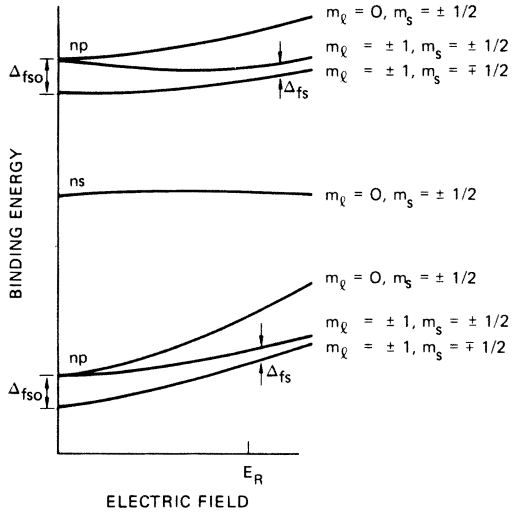

FIG. 10. The fine-structure levels in zero field and at the field of the collisional resonances.

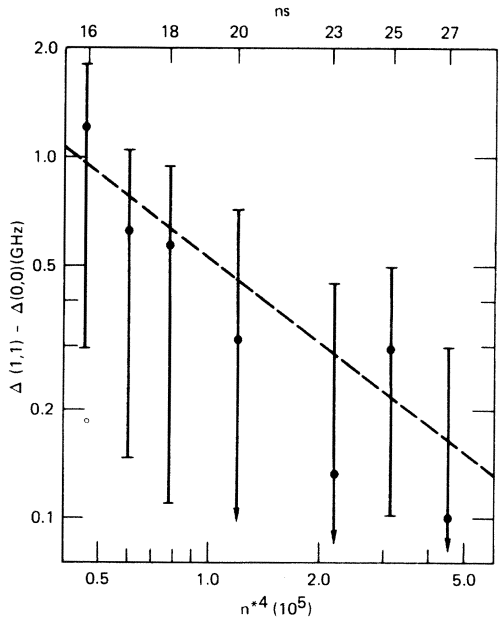

FIG. 11. The difference in widths of the 1,1 and 0,0 resonances (●) and a plot of the calculated value of Δ_{fs} (— — —).

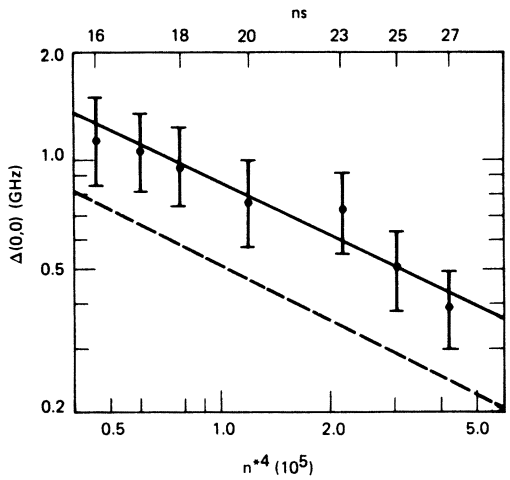

FIG. 12. The widths of the 0,0 resonances (●), the fit curve (—), and a plot of the calculated dependence (– – –).

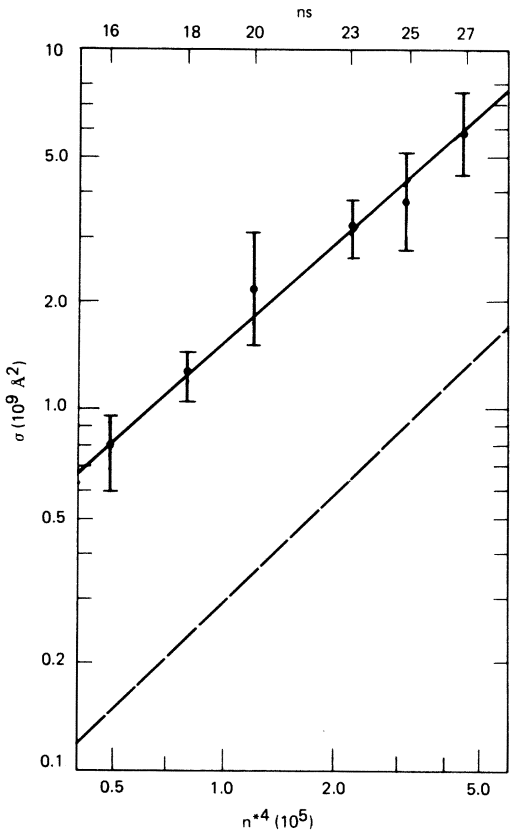

FIG. 13. The observed cross sections with their relative error bars (●), the fit curve (—), and the calculated dependence (– – –).

tions such as far-infrared or microwave detection requiring samples of Rydberg atoms which are somewhat dense.[25–28] While at first such processes appear to be a nuisance, it may be possible to put the effect to good use.

ACKNOWLEDGMENTS

It is a pleasure to acknowledge stimulating and helpful conversations with W. E. Cooke, R. M. Hill, T. Oka, B. R. Junker, S. E. Harris, and J. Briggs in the course of this work, which was supported by the Office of Naval Research under Contract No. N00014-79-C-0212.

APPENDIX

To convert the widths from their field values to frequency we use the following approach.[29] In Fig. 14 we show the atomic levels in an electric field.

TABLE IV. Radiative lifetimes, relative and absolute cross sections.

State	Lifetime[a] (μsec)	$N_p'/N_s'^2$ (Relative cross section) (10^9 C^{-1})	σ (10^9 Å^2)
16s	4.34	1.45(35)	0.78(18)
18s	6.37	2.31(23)	1.25(13)
20s	8.96	4.0(12)	2.16(66)
23s	14.0	6.0(9)	3.2(5)
25s	18.3	7.1(19)	3.8(10)
27s	23.3	10.7(33)	5.8(18)

[a]See Ref. 22.

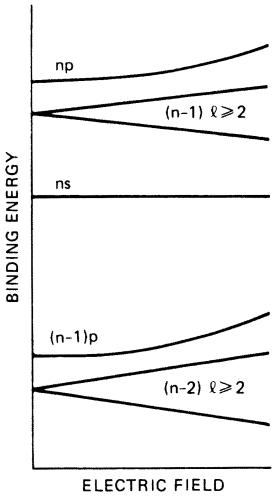

FIG. 14. Energy levels of the Rydberg states in an electric field, showing the Stark shifts of the *s*,*p*, and hydrogenic $l \geq 2$ states.

The position of the *s* state is essentially independent of field in the region shown so we shall assume it has zero Stark shift. Note that the *p* states are displaced from the hydrogenic position by an amount $\Delta p = \delta p / n^3$ in zero field and exhibit a linear Stark shift $\sim n^2 E$ at high field. This suggests that the Stark shift W_p of a *P* state be written as

$$W_p = (\Delta p^2 + n^4 E^2)^{1/2} - \Delta p \ . \tag{A1}$$

The *average* stark shift of the two *p* states may be written as

$$\overline{W}_p = (\Delta p^2 + n^{*4} E^2)^{1/2} - \frac{\delta p}{n^{*3}} \ , \tag{A2}$$

where for n^* we use the effective quantum number of the *s* state which lies halfway between the two *p* states. The slope of this curve yields the desired conversion of widths from fields to frequencies. Explicitly

$$\frac{d\overline{W}_p}{dE} = \frac{n^{*4} E}{(\delta p / n^{*3} + n^{*4} E^2)^{1/2}} \ . \tag{A3}$$

We are, of course, interested in this value at the resonances for which the average value of the energies of the two *p* states above and below the *s* states equals the energy of the *s* state. If Δ_0 is the amount by which the average of the two *p* state energies lies below the *s* state energy, then at resonance $\overline{W}_p = \Delta_0$. From the spectroscopy of the Na *s* and *p* states $\Delta_0 = M n^{*-3.73}$ where $M = 0.236$.[30] Thus at resonance the average field E_R must satisfy

$$\left[\left[\frac{\delta p}{n^{*3}} \right]^2 + n^4 E_R^2 \right]^{1/2} - \frac{\delta p}{n^{*3}} = \frac{M}{n^{*3.73}} \ . \tag{A4}$$

In fact the two sides of Eq. (A4) are equal to 10% justifying the approximation of Eq. (A1).

Equation (A3) can be rewritten for $E = E_R$

$$\left. \frac{d\overline{W}_p}{dE} \right|_{E_R} = \frac{n^{*4} E_R}{\delta p / n^{*3} + M / n^{*3.73}} \ . \tag{A5}$$

Since E_R for the (0,0) resonance is given by $E_R = Q_n^{*-5.35}$, with $Q = 0.236$, we can write Eq. (A5) as

$$\left. \frac{d\overline{W}_p}{dE} \right|_{E_R} = \frac{Q n^{*-1.35}}{\delta p / n^{*3} + M / n^{*3.73}} \ . \tag{A6}$$

We may rewrite Eq. (A6) as

$$\left. \frac{d\overline{W}_p}{dE} \right|_{E_R} = \frac{Q n^{*1.65}}{\delta p + M n^{*-0.73}} \ . \tag{A7}$$

If we replace $M n^{*-0.73}$ by its average value, 0.027, over the range of *n* studied we can rewrite Eq. (A7) with 3% accuracy as

$$\left. \frac{d\overline{W}_p}{dE} \right|_{E_R} = 1.33 n^{*1.65} \ . \tag{A8}$$

We may express Eq. (A8) in more practical units as

$$\Delta \overline{W}_p (\text{GHz}) = 1.72 \times 10^{-3} n^{*1.65} \Delta E \ (\text{V/cm}) \ . \tag{A9}$$

Since the frequency of the *ns*-*np* transition is shifted up at the rate given by Eq. (A9) while the frequency of the *ns*-$(n-1)p$ transition is shifted down by the same rate, the width Δ of the collisional resonances is twice as large as shown by Eq. (A9).

$$\Delta (\text{GHz}) = 3.44 \times 10^{-3} n^{*1.65} \Delta E \ (\text{V/cm}) \ . \tag{A10}$$

*Permanent address: Schlumberger-Doll Research, Ridgefield, Conn. 06877.
†Permanent address: CEN Saclay, Service de Physique des Atomes et des Surfaces, 91191 Gif-sur-Yvette, Cedex, France.
‡Permanent address: Institut d'Electronique Fondamental, 91405 Orsay, France.
§Permanent address: Fakultat für Physik, 3 Herman Herder Strasse, D7800 Freiburg, West Germany.

[1]N. F. Mott and H. S. W. Massey, *The Theory of Atomic Collisions* (Clarendon, Oxford, 1950).
[2]P. W. Anderson, Phys. Rev. 76, 647 (1949).
[3]J. van Kranendonk, Can. J. Phys. 41, 433 (1963).
[4]T. Oka, in *Advances in Atomic and Molecular Physics,* edited by D. R. Bates and I. Esterman (Academic, New York, 1973), Vol. 9.
[5]P. L. Houston, in *Photoselective Chemistry, Part 2,* edited by J. Jortner (Wiley, New York, 1981).
[6]K. A. Smith, F. G. Kellert, R. D. Rundel, F. B. Dunning, and R. F. Stebbings, Phys. Rev. Lett. 40, 1362 (1978).
[7]T. H. Jeys, G. B. McMillan, K. A. Smith, F. B. Dunning, and R. F. Stebbings, Proceedings of the Twelfth ICPEAC, 1981, p. 1107 (unpublished).
[8]T. F. Gallagher, G. A. Ruff, and K. A. Safinya, Phys. Rev. A 22, 843 (1980).
[9]K. A. Safinya, J. F. Delpech, F. Gounand, W. Sandner, and T. F. Gallagher, Phys. Rev. Lett. 47, 405 (1981).
[10]G. E. Pake, *Paramagnetic Resonance* (Benjamin, New York, 1962).
[11]E. M. Purcell, Astrophys. J. 116, 457 (1952).
[12]N. F. Ramsey, *Molecular Beams* (Oxford University Press, London, 1956).
[13]D. Kleppner, in *Atomic Physics and Astrophysics,* edited by M. Chrétien and E. Lipworth (Gordon and Breach, New York, 1971).
[14]T. F. Gallagher, L. M. Humphrey, W. E. Cooke, R. M. Hill, and S. A. Edelstein, Phys. Rev. A 16, 1098 (1977).
[15]D. C. Lorents, D. J. Eckstrom, and D. L. Huestis, SRI Report No. MP 73-2 (unpublished).
[16]M. Gross, C. Fabre, P. Goy, S. Haroche, and J. M. Raimond, Phys. Rev. Lett. 43, 343 (1979).
[17]J. C. MacGillivray and M. S. Feld, Phys. Rev. A 14, 1169 (1976).
[18]R. Freidberg, S. R. Hartmann, and J. T. Manassah, Phys. Lett. 40A, 372 (1972).
[19]N. E. Rehler and J. H. Eberly, Phys. Rev. A 3, 1735 (1971).
[20]W. E. Cooke (private communication).
[21]T. F. Gallagher, L. M. Humphrey, R. M. Hill, W. E. Cooke, and S. A. Edelstein, Phys. Rev. A 15, 1937 (1977).
[22]F. Gounand, J. Phys. (Paris) 40, 457 (1979).
[23]W. E. Cooke and T. F. Gallagher, Phys. Rev. A 21, 588 (1980).
[24]R. W. Falcone, W. R. Green, J. C. White, J. F. Young, and S. E. Harris, Phys. Rev. A 15, 1333 (1977).
[25]D. Kleppner, and T. W. Ducas, Bull. Am. Phys. Soc. 21, 600 (1976).
[26]T. F. Gallagher and W. E. Cooke, Appl. Phys. Lett. 34, 369 (1979).
[27]T. Ducas, W. Spencer, A. Vaidyanathan, W. Hamilton, and D. Kleppner, Appl. Phys. Lett. 35, 382 (1979).
[28]H. Figger, G. Leuchs, R. Straubinger, and H. Walther, Opt. Commun. 33, 37 (1980).
[29]W. E. Cooke (private communication).
[30]C. Fabre, These de Doctor d'Etat, Université Pierre et Marie Curie, Paris, France, 1980 (unpublished).